ISPRS Journal of Photogrammetry and Remote Sensing 141 (2018) 148–160

Contents lists available at ScienceDirect

ISPRS Journal of Photogrammetry and Remote Sensing

journal homepage: www.elsevier.com/locate/isprsjprs

Dynamics of the wetland vegetation in large lakes of the Yangtze Plain in response to both fertilizer consumption and climatic changes

Xuejiao Hou[a,b], Lian Feng[a,c,d,*], Xiaoling Chen[b], Yunlin Zhang[c]

[a] School of Environmental Science and Engineering, Southern University of Science and Technology of China, Shenzhen 518055, China
[b] State Key Laboratory of Information Engineering in Surveying, Mapping and Remote Sensing, Wuhan University, Wuhan 430079, China
[c] State Key Laboratory of Lake Science and Environment, Nanjing Institute of Geography and Limnology, Chinese Academy of Sciences, Nanjing 210008, China
[d] Guangdong Provincial Key Laboratory of Soil and Groundwater Pollution Control, School of Environmental Science and Engineering, Southern University of Science and Technology, Shenzhen 518055, China

ARTICLE INFO

Keywords:
Wetland vegetation
Yangtze Plain
Lakes
MODIS
Time series
Fertilizer consumption

ABSTRACT

Using moderate-resolution imaging spectroradiometer (MODIS) data that cover the 15-year period from 2000 to 2014 and a phenology-based classification method, the long-term changes in the wetland vegetation of 25 large lakes on the Yangtze Plain were obtained. The classification method was developed based on the phenological information extracted from time series of MODIS observations, which demonstrated mean user's/producer's accuracies of 76.17% and 84.58%, respectively. The first comprehensive record of the spatial distribution and temporal dynamics of wetland vegetation in the large lakes on the Yangtze Plain was created. Of the 25 lakes examined, 17 showed a decreasing trend of vegetation area percentages (VAPs) during the study period, and 7 were statistically significant ($p < 0.05$). The same number of lakes was found to display decreasing trends in vegetation greenness over this 15-year period, and these decreasing trends were statistically significant ($p < 0.05$) for 11 of the lakes. Substantially fewer lakes showed increases in either their VAPs or their vegetation greenness values. Analysis using a multiple general linear model revealed that the amounts of chemical fertilizer used for farmlands surrounding the lakes, precipitation, daily sunshine hours, temperature and water turbidity played the most important roles in regulating the interannual changes in vegetation greenness in 40% (10/25), 12% (3/25), 4% (1/25), 20% (5/25) and 12% (3/25) of the lake wetlands, respectively. On average, the combined effects of these five driving factors above explained 89.08 ± 7.89% of the variation in greenness over this 15-year period for the 25 lakes. This wetland vegetation environmental data record (EDR) of large lakes in Yangtze Plain demonstration will provide a crucial baseline information for the wetland environment conservation and restoration.

1. Introduction

As one of the most important components of wetland ecosystems, vegetation plays important roles that include providing food and habitat for aquatic organisms, maintaining water quality, and storing carbon (Scheffer et al., 1993; Jeppesen et al., 1998; Xiao et al., 2015). Changes in wetland vegetation have been considered a key ecological indicator for transitions in the safety and sustainability of the water environment (Martin et al., 2010; Feng et al., 2016; Zhang et al., 2016a). Unfortunately, global wetland vegetation loss is accelerating (Zhang et al., 2017a), mainly due to stress from anthropogenic activities, such as aquaculture and reclamation, as well as climate extremes (floods, etc.) and global warming (Sand-Jensen et al., 2000; Short et al., 2016), which will cause numerous environmental problems and have an adverse impact on ecological functions. The wetlands of the inland lakes on the Yangtze Plain examined in this study are susceptible to these problems (Han et al., 2015; Song et al., 2016; Zhang et al., 2016b).

Accurate knowledge of the distribution changes of wetland vegetation is the first step in assessing potential changes in the ecological functions of wetlands. Mapping the spatial patterns of vegetation in large wetland systems is often challenging, due to the heterogeneous distributions and compositions of different wetland cover types (Houlahan et al., 2006; Szantoi et al., 2013). Traditional field surveys can provide accurate data, but they are always labor and time intensive, and for the phenological change of wetland vegetation, frequent field measurements should be taken to obtain updated information to monitor wetland changes effectively, which will be more time-

* Corresponding authors at: School of Environmental Science and Engineering, Southern University of Science and Technology of China, Shenzhen 518055, China.
E-mail address: fengl@sustc.edu.cn (L. Feng).

https://doi.org/10.1016/j.isprsjprs.2018.04.015
Received 30 January 2018; Received in revised form 13 April 2018; Accepted 20 April 2018

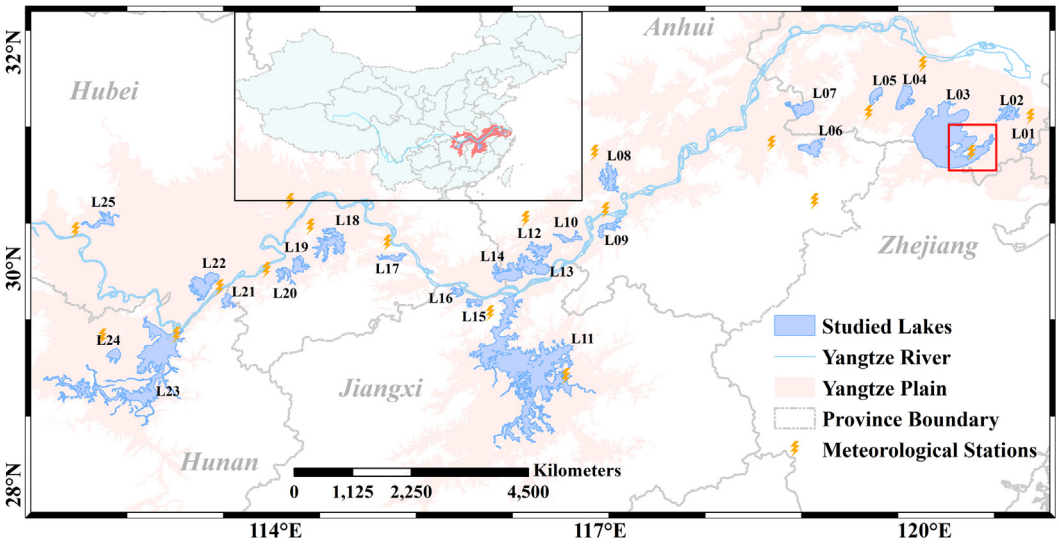

Fig. 1. Hydrological map of the Yangtze Plain (pink shaded area) and the spatial distribution of the studied lakes. The locations of meteorological stations are indicated by the orange markers, where ground-based measurements were used to assess the driving factors affecting the wetlands. The location of the Yangtze Plain in China is shown in the inset. (For interpretation of the references to color in this figure legend, the reader is referred to the web version of this article.)

consuming and expensive (Ozge et al., 2009; Han et al., 2015). As such, it is very difficult to collect spatially and temporally representative vegetation records for the wetland systems of large lakes across the entire Yangtze Plain or understand the changes in vegetation in this region using field surveys.

Given their ability to collect synoptic observations frequently, remote sensing techniques have become effective tools in studying wetland vegetation (Li et al., 2013; Han et al., 2015; Luo et al., 2016; Chen et al., 2018). Satellite remote sensing imagery with spatial resolutions ranging from < 10 m (such as Quickbird, IKONOS, Unmanned Aerial Vehicle, SAR images) to several kilometers have been used worldwide to map wetland vegetation (Ozge et al., 2009; Laba et al., 2010; Yu and Hu, 2013; Betbeder et al., 2015; Jing et al., 2017; Liu and Abd-Elrahman, 2018). The methods used to classify wetland vegetation from remote sensing images have also evolved from visual interpretation to computerized methods (i.e., the threshold method, unsupervised and supervised classification, Object-based classification, principal component analysis and hybrid classification) and subsequently to highly advanced artificial intelligence-based methods (Maxa and Bolstad, 2009; Wang and Bao, 2010; Dronova et al., 2015; Szantoi et al., 2015; Villa et al., 2015; Liu and Abd-Elrahman, 2018). Several studies also try to estimate the coverage and community of wetland vegetation using remote sensing imagery (Ozge et al., 2009; Laba et al., 2010; Dronova et al., 2015; Villa et al., 2015), and in situ data were used to train model and validate accuracy.

The lakes, ponds and reservoirs on the Yangtze Plain account for over three-quarters of the freshwater lake area in the downstream portion of the Yangtze Basin, where the wetlands can provide water resources for millions of local people and play critical roles in regulating the regional environmental and ecological systems (Guo, 2007; Han et al., 2015). Indeed, considerable efforts have been made to understand the changes in the surface area, land cover, and water quality of these lakes, among many other characteristics (Feng et al., 2012a, 2012b; Wang et al., 2014, 2017; Cai et al., 2016; Hou et al., 2017; Xie et al., 2017). The wetland vegetation of large lakes in this region has also been studied in a number of pioneering studies starting in the 1970s, such as Poyang Lake, Dongting Lake, etc. (Wu, 1977; Liu et al., 1981; Deng et al., 2014; Luo et al., 2017; Chen et al., 2018).

Unfortunately, published studies of the wetland vegetation of the Yangtze Plain have several limitations. First, some of these studies use data from only one to two years, which prevents the analysis of long-term changes and their potential trends (Luo et al., 2017). Second, some of the studies conducted with remote sensing data covering longer periods suffer from nonconsecutive observations, which prevent the assessment of short-term vegetation variability (Li et al., 2013; Han et al., 2015). Third, the available information on wetland vegetation provided by field surveys and remote sensing focuses only on one lake in the Yangtze Plain, prohibiting comprehensive assessment of the basin-scale wetland conditions (Luo et al., 2016; Chen et al., 2018; Han et al., 2018). Prompted by the urgent need for an accurate decadal environmental data record (EDR) of the wetland vegetation of the inland lakes of the Yangtze Plain, the current study is designed to address the issues described above. The objectives of the study are as follows: (1) To develop a phenology-based classification method using time series of the 250-m moderate-resolution imaging spectroradiometer (MODIS) data and to document the spatial and temporal variability of the vegetation changes in 25 large lakes on the Yangtze Plain between 2000 and 2014; (2) To explore the potential driving forces of the changes in greenness in these wetlands using anthropogenic activities data, meteorological and water quality data obtained through both ground-based measurements and remote sensing.

2. Study area and datasets

2.1. Study area

The Yangtze Plain, which covers an area of ~140,000 km^2 (see Fig. 1), accounts for ~18% of the total area of the downstream Yangtze Basin (Wang et al., 2014). The freshwater lakes in this region include those connected with the Yangtze River (such as Poyang, Dongting, and Shijiu Lake), whose intra-annual changes in their inundation areas are impacted by the Yangtze River (Feng et al., 2012a; Wang et al., 2014), as well as those that have no direct interaction with the Yangtze River. However, due to the increase in anthropogenic activities, many lake wetlands have experienced significant degradation over the past several decades (Ma et al., 2008; Zhang et al., 2016a, 2016b). Recently, a new review paper by Zhang et al. (2017a) stated that of the 35 lakes with aquatic vegetation loss in China, many were distributed in the Yangtze Plain. However, hitherto no systematic reports on the long-term wetland vegetation changes in the Yangtze Plain are available, while information on these changes is critical for protection and restoration of the lake environment. Notably, the words “lake” and “wetland” are interchangeable in this study, as lake is also one type of wetland according to the definition of Ramsar convention (Secretariat, 2013)

Table 1
The codes, names, locations and water areas (which have inundation probabilities of > 80% between 2000 and 2014) of the studied lakes. Also listed are the 15-year annual mean vegetation area percentages (VAPs), greenness values and their corresponding standard deviations for each lake, which were derived from the MODIS data.

Code	Name	Lon.	Lat.	Area (km^2)	VAPs (%)		Greenness	
					Ave.	Std.	Ave.	Std.
L01	Dianshan	120.96	31.12	75.2	24.43	3.09	0.10	0.02
L02	Yangcheng	120.77	31.43	154.9	46.78	6.79	0.20	0.03
L03	Taihu	120.19	31.20	880.3	25.78	2.91	0.14	0.02
L04	Gehu	119.81	31.60	231.7	38.30	7.48	0.18	0.05
L05	Changdang	119.55	31.62	106.8	40.55	5.92	0.20	0.04
L06	Nanyi	118.96	31.11	205.4	33.27	4.13	0.17	0.02
L07	Shijiu	118.88	31.47	248.7	39.74	16.08	0.18	0.07
L08	Caizi	117.07	30.80	213.5	43.99	7.99	0.22	0.04
L09	Shengjin	117.07	30.38	117.9	52.36	8.64	0.24	0.05
L10	Qingcao	116.69	30.28	75.6	38.37	4.28	0.19	0.03
L11	Poyang	116.32	29.08	3497.8	40.45	9.45	0.25	0.04
L12	Bohu	116.44	30.17	147.5	23.64	4.56	0.10	0.02
L13	Huangda	116.38	30.02	279.7	35.09	8.74	0.23	0.08
L14	Longgan	116.15	29.95	293.4	29.31	5.57	0.19	0.04
L15	Saihu	115.85	29.69	58.7	38.92	3.43	0.16	0.02
L16	Chihu	115.69	29.78	50.8	58.89	6.79	0.27	0.04
L17	Daye	115.10	30.10	81.7	46.96	6.36	0.21	0.04
L18	Liangzi	114.51	30.23	342.4	38.38	5.66	0.18	0.03
L19	Futou	114.23	30.02	138.8	41.30	6.22	0.22	0.05
L20	Xiliang	114.08	29.95	96.4	58.49	4.70	0.27	0.03
L21	Huanggai	113.55	29.70	85.1	51.15	8.20	0.22	0.04
L22	Honghu	113.34	29.86	376.5	44.31	9.02	0.23	0.05
L23	Dongting	113.12	29.34	1990.5	52.75	7.70	0.33	0.03
L24	Datong	112.51	29.21	91.1	16.78	1.84	0.08	0.02
L25	Changhu	112.40	30.44	154.4	51.71	4.48	0.22	0.04

Here, we focus on the changes in wetland vegetation that have occurred in the lakes with surface areas of > 50 km^2 on the Yangtze Plain (except for Chaohu Lake), considering the moderate resolution of the MODIS data and the limited detectability of smaller lakes. A total of 25 lakes were examined, and the surface area of these lakes accounts for ~87% of the total inland waters in the Yangtze Plain (estimated from Wang and Dou (1998) and Liu et al. (2008)). Table 1 displays the codes, names, locations (latitude and longitude), and surface areas (i.e., the areas with inundation probabilities of > 80% between 2000 and 2014) of these lakes. The code numbers were assigned to these lakes based on their longitudes, and the numbers increase from east to west within the Yangtze Plain (see Fig. 1). Note that Chaohu Lake (which has a surface area of 769.55 km^2) and the western part of Taihu Lake were excluded from consideration in this study. Heavy algal blooms occur frequently in these areas (Hu et al., 2010; Zhang et al., 2015), and it is difficult to discriminate between floating algae and wetland vegetation in those regions by the method used in this study.

2.2. Datasets

1366 MODIS/Terra 250-m 8-day surface reflectance products between 2000 and 2014 were downloaded from the NASA Land Processes Distribution Active Archive Center (https://ladsweb.nascom.nasa.gov/) and were used to classify the wetland cover types, the Normalized Difference Vegetation Index (NDVI) was calculated for the data from each 8-day period, and the Harmonic Analysis of Time Series (HANTS) method was applied to the annual NDVI series to fill in the gaps caused by the excluded low quality data and to remove potential noise on the temporal scale (Verhoef, 1996). 105 Landsat TM, ETM+ and OLI surface reflectance products during both dry and wet seasons from 2000 to 2014 on the Yangtze Plain were obtained from the Landsat Data Access (https://landsat.usgs.gov/landsat-data-access) and were used to assess the accuracy of the wetland vegetation classification obtained using the 250-m-resolution MODIS products.

Monthly air temperatures and data on the number of sunshine hours each day were obtained from the China Meteorological Data Sharing Service System (http://data.cma.gov), where the data collected from the nearest meteorological stations (see Fig. 1) were used to represent the weather conditions for individual lakes. The precipitation data used in this work represent monthly composites of Tropical Rainfall Measuring Mission data (TRMM 3B43), which were obtained from the NASA Goddard Distributed Active Archive Center (DAAC) (http://trmm.gsfc.nasa.gov/). The monthly TRMM data have been validated in this region, and they show excellent agreement with ground-based measurements (Duan et al., 2012; Feng et al., 2012a). Each grid cell of the TRMM data represents an area of 0.25° × 0.25° (~25 × 25 km at the equator). The cells that overlap with individual lakes were extracted, and the mean values were used to represent the precipitation conditions for that lake.

MODIS-derived water turbidity parameters (i.e., the concentrations of total suspended sediments or TSS) were used to study the responses of wetland vegetation to water clarity in this study, the data collection was described in Hou et al. (2017).

The amounts of yearly used chemical fertilizer for farmlands surrounding each lake, represented as the integration of the counties round the lake, were obtained from the local annual statistical books (Anhui, 2001–2015; Hunan, 2001–2015; Hunbei, 2001–2015; Jiangsu, 2001–2015; Jiangxi, 2001–2015; Zhejiang, 2001–2015) and were used to investigate the influence of anthropogenic activities on wetland vegetation changes.

3. Methods

3.1. Determination of lake boundaries

Before the wetlands associated with the studied lakes could be classified into different cover types, the boundary for each lake needed to be determined. We defined the wetlands associated with these lakes using the MODIS time series data as follows. Pixels that had an inundation frequency of > 80% in the MODIS 8-day composites (i.e., for every 100 MODIS composites, 80 were classified as water for that pixel) over the 15-year study period were classified as wetlands, and the maximum range of such pixels surrounding a given lake was considered to represent the wetland boundary of that lake. This definition generally follows the Ramsar convention (Secretariat, 2013), and the boundary for each lakes was fixed during the 15 years. The inundation area for each MODIS 8-day composite was delineated using a semi-automatic method that employed NDWI (Normalized Difference Water Index, $NDWI = (R_{green} - R_{nir})/(R_{green} + R_{nir})$) data and a self-developed graphical user interface (GUI). This approach was similar to the inundation extraction approach used in Hou et al. (2017). The boundaries of the 25 selected lakes are shown in Fig. 1. Note that the boundary for Taihu Lake was confined to a region of interest (ROI) in the eastern part of the lake.

3.2. Analysis of the spectral and temporal features of different vegetation categories

Three major cover types, vegetation, water and mudflats, can be found in the wetlands associated with the selected lakes, and the first step of our study was to select an effective method to distinguish vegetation from the other two types for all 25 lakes with different changes in the water environment (i.e., seasonal inundation change). Image classification methods, such as supervised/unsupervised classification, had been used to discriminate the wetland vegetation from the other two types using remote sensing observations (Ozge et al., 2009; Han et al., 2015). Unfortunately, such methods could not be applied in this study because the MODIS 250-m 8-day composite includes only two wavelengths that are centered on 645 and 859 nm, where the spectral information may not be sufficient to separate three different cover types

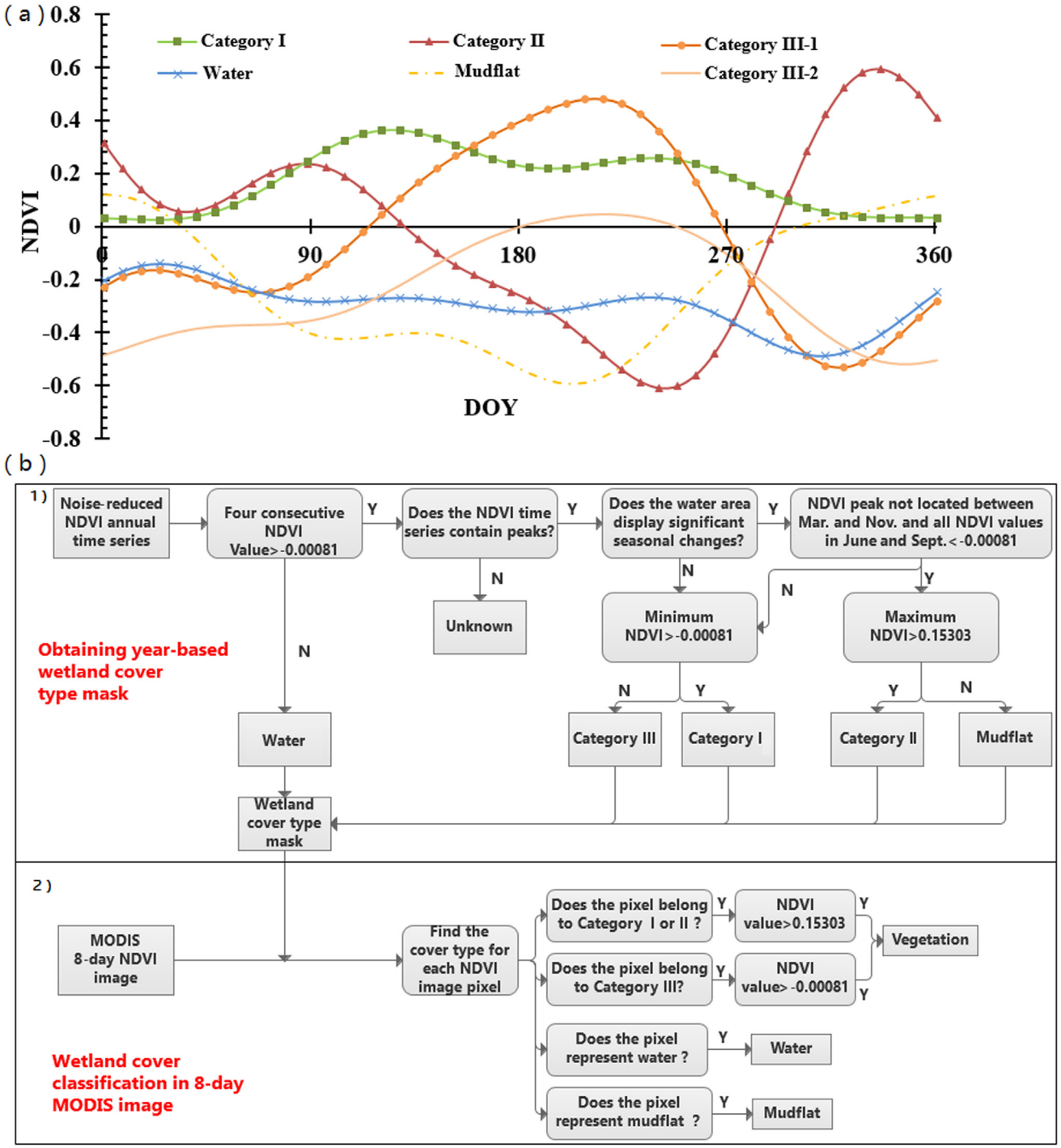

Fig. 2. (a) Annual NDVI series (derived using MODIS 8-day composites) of different wetland cover types. Categories I to III represent vegetation with different growing conditions (Fig. 3), Categories III-1 and III-2 showed two typical conditions of Category III. (b) The flowchart of the method used for wetland vegetation classification. (1) Workflow used to generate the year-based possible vegetation occurrence mask using the NDVI series in each year. (2) Workflow of using the year-based possible vegetation occurrence mask to perform vegetation classification for each 8-day NDVI composite.

using these computerized classification methods. Additionally, a NDVI threshold approach could be used to separate vegetation from other cover types (Patel et al., 2015), as vegetation often shows much higher NDVI values than water and mudflats. Such methods typically work well for vegetation in floodplains of some lakes under conditions with decreased water levels. Unfortunately, low NDVI values may also be associated with submerged vegetation in some lakes with abundant water. The NIR band is absorbed much more strongly in water than the red band, resulting in NDVI values of mixed water and submerged plants may be smaller than those of exposed mudflats (see Categories III-2 and Mudflat in Fig. 2a).

The challenges associated with using a single NDVI threshold can be revealed through examination of the annual noise-reduced NDVI curves shown in Fig. 2a. These curves in Fig. 2a represent the typical variations in annual NDVI for the different cover types found in association with the 25 studied lakes shown in Fig. 1, the magnitudes and patterns may vary with location and year. Indeed, even if the NDVI values of Category III-2 (Figs. 2a and 3d) were very small throughout a year, high-

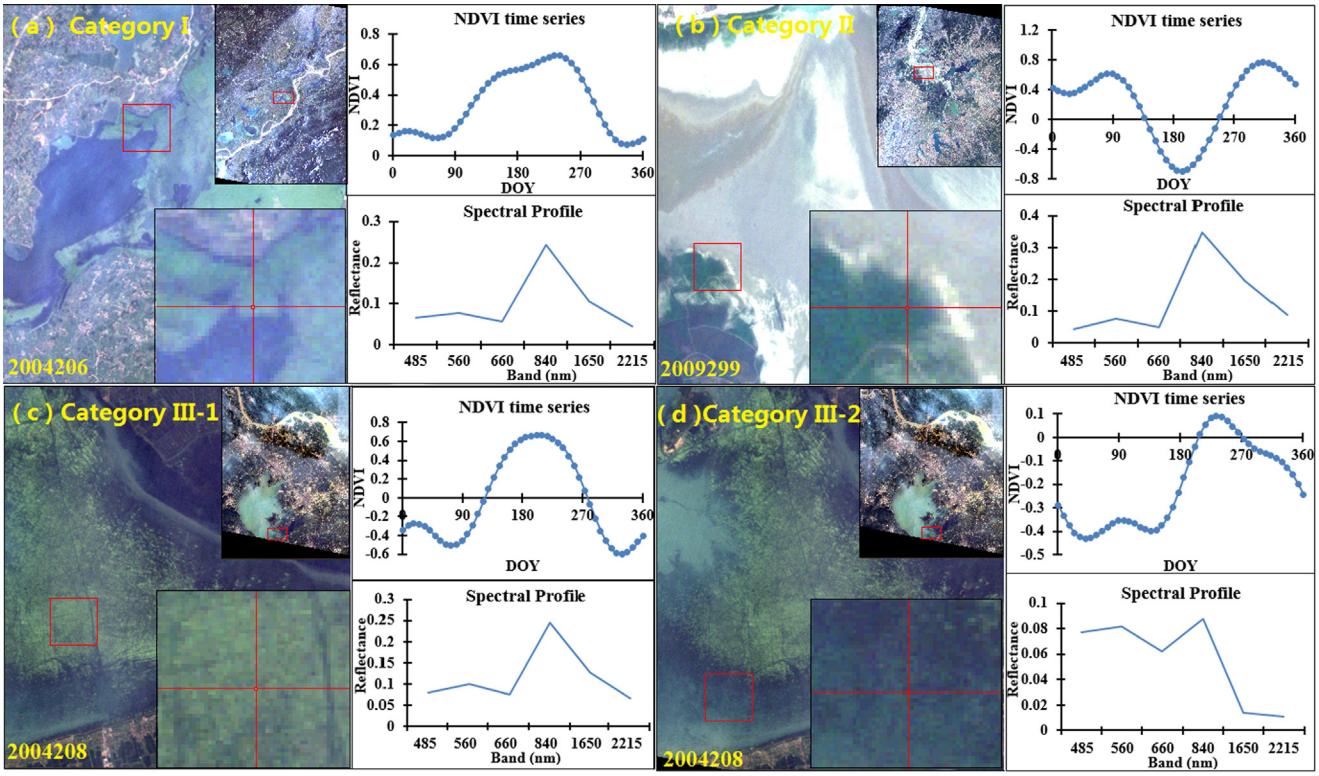

Fig. 3. Typical examples to illustrate vegetation Categories I (a, in Qingcao Lake), II (b, in Poyang Lake), III-1 and III-2 (c, d, in Taihu Lake). The spectral profiles of the cross-located pixels were obtained from Landsat surface reflectance products, and the annual NDVI time series were from MODIS data of the same locations. The RGB true color images were composed using Landsat data, where acquisition dates were also annotated.

resolution images collected in the same year indicated the presence of vegetation in the summer. On the other hand, mudflat showed positive NDVI values during particular periods (winter), whereas it manifested as mudflats in high-resolution images over the entire year. As such, large errors would be expected if a simple NDVI threshold method were used to delineate vegetation in these images.

When analyzing the annual NDVI series, the diversity of phenological features between the different cover types represent useful information that can be used to help improve the vegetation classification accuracy. We examined the wetland vegetation of all 25 lakes, and the annual NDVI changes of vegetation generally fell into three categories. As shown in Fig. 2a, these three categories demonstrated prominent increasing trends in their NDVI values during certain parts of the year. Category I showed positive NDVI values for most of the year (see Fig. 2a and 3a), where the NDVI values displayed an increasing trend over the growing season. Wetland vegetation with this type of growing curve was generally found in the near-shore regions of the lakes or along bare lake bottom (Fig. 3a), where the seasonality of the NDVI values was generally caused by the phenology of the vegetation. The second category (Category II) of vegetation was only found in lakes with substantial intra-annual changes in their inundation areas (such as Poyang Lake) (see Figs. 2a and 3b). This category was only observed in the floodplains of dynamic lakes (i.e., Poyang Lake and Dongting Lake) where the water retreated during the dry seasons, and the vegetation became submerged when the water level increased during the wet seasons, producing negative NDVI values. Category III reflects a rapid increase in NDVI values during the warm seasons of vegetation growth and negative NDVI values in the cold seasons (Fig. 2a, Categories III-1 and III-2 and Fig. 3c and d). This category of vegetation was often found living in or above water, and two types of vegetation might result in such annual NDVI patterns. (1) The vegetation either died or manifested as submerged plants during the cold non-growing seasons and then germinated and grew out of the water during the warm growing seasons. (2) Floating aquatic macrophytes, which generally grew during the warm seasons and died during the cold seasons, could also be responsible for this pattern. Therefore, small NDVI values could be found for Category III, which even appeared in the summer (Category III-2, in Fig. 3d), due primarily to its proximity to water, while the NDVI values associated with Categories I and II would show high values when vegetation was present. In contrast, the NDVI values of areas permanently covered by water were negative throughout the year (Water in Fig. 2a), and no significant increase in the NDVI in the growing season could be observed for permanent mudflats over the course of the year (Mudflat in Fig. 2a).

3.3. Classification of wetland vegetation

A possible vegetation occurrence mask was generated for each year based on the above phenological analysis (Fig. 2b). Specifically, we would not expect to see any vegetation growth over the course of a year in areas with NDVI annual patterns that mimic those of water and mudflat, and the 8-day MODIS composite during the entire year should be classified as non-vegetation for these areas. Pixels with NDVI patterns that followed Categories I, II or III were considered to indicate the vegetation mask, where green vegetation could be present during certain parts of the year. and with the year-based vegetation mask, a NDVI threshold could be used to differentiate the vegetation and the other cover types in the 8-day MODIS data to obtain the 8-day vegetation distribution information. The possible vegetation occurrence mask was generated as follows: Pixels without NDVI values > -0.00081 in four consecutive 8-day MODIS composites were masked as water in that year (we assumed that any green wetland vegetation was present for at least one month). Otherwise, the annual NDVI time series was examined to determine whether any NDVI peak was present in a given year. Pixels were masked as possible vegetation if a peak was present; otherwise, they were considered as unknown. According to the seasonal inundation

changes of lakes, the NDVI time series of the possible vegetation pixels were classified into different categories, and the vegetation classification methods differed for lakes with and without significant seasonal inundation changes. For the former cases, a minimum annual NDVI threshold ($NDVI_{annual\_minima}$) was used to separate the annual NDVI curves belonging to Categories I ($NDVI_{annual\_minima} > -0.00081$) and III ($NDVI_{annual\_minima} < -0.00081$). For the lakes that displayed dynamic inundation (i.e., Poyang and Dongting Lakes), if the annual NDVI peak was located between March and November, and the NDVI values were > -0.00081 during June and September, the vegetation classification was conducted in a similar way to that of the lakes without significant inundation seasonality. Otherwise, a maximum annual NDVI threshold ($NDVI_{annual\_maximum}$) was used to separate the annual NDVI curves belonging to Categories I ($NDVI_{annual\_maximum} > 0.15303$) and mudflat ($NDVI_{annual\_maximum} < 0.15303$). The workflow of the possible vegetation occurrence mask is demonstrated in Fig. 2b(1).

This year-based possible vegetation occurrence mask was used to differentiate the wetland vegetation of the selected lakes from areas of mudflat and water for each 8-day MODIS composite to obtain the 8-day vegetation distribution information (see Fig. 2b(2)). Specifically, if a location was masked as water or mudflat in the possible vegetation occurrence mask, it would be excluded from further vegetation detection for all the 8-day MODIS composites corresponding to that year. On the other hand, although vegetation could be observed in locations that were masked as possible vegetation (i.e., annual NDVI curves similar to Categories I, II, and III), the NDVI thresholds used to separate vegetation from its background, as noted above. In practice, for areas masked as Categories I and II in the possible vegetation occurrence mask with the annual NDVI series, if a pixel in a MODIS 8-day composite had a NDVI value > 0.15303, it was classified as vegetation in these 8-day data. For regions masked as Category III, a NDVI threshold of > -0.00081 was used to identify the vegetation in each MODIS 8-day composite.

The thresholds (-0.00081 and 0.15303) used here were determined as follows: pre-classified Landsat maps with three cover types (water, mudflat and vegetation) were obtained first (see below for details of the Landsat classification), which were considered error-free data. Then, > 10,000 random points of both water and mudflats classes were selected from these Landsat classification maps from all 25 lakes of both dry and wet seasons. Concurrent MODIS NDVI data of these points (i.e., same location and time) were used to generate histograms. The histogram mode of water (i.e., -0.00081) was determined to separate vegetation from the water background and mudflats, while the mode of mudflats (i.e., 0.15303) was then used for the discrimination of vegetation and mudflats. Indeed, tests indicated that the vegetation change trends of all the studied lakes were insensitive to these thresholds.

Both the generation of the possible vegetation occurrence mask and the vegetation discrimination were repeated for all the observed years, and the vegetation coverage was obtained for each of the 8-day MODIS composites between 2000 and 2014.

3.4. Assessment of the wetland vegetation changes

Two parameters were used to assess the wetland vegetation conditions and the corresponding interannual dynamics in the selected lakes. The first parameter is the vegetation area percentage (VAP), which is defined as the percentage of the vegetation cover that accounts for the total area of a lake wetland (which is the area with an inundation probability of > 80% between 2000 and 2014; see Table 1). The second parameter is the vegetation greenness, which is represented by the mean NDVI value of the area identified as vegetation in a lake in each 8-day MODIS composite. Note that the VAP mainly represents the vegetation coverage, while greenness reflects the growing status. The seasonal VAPs and greenness values were calculated for each lake, and these values were used to estimate the annual mean conditions. To avoid impacts of seasonal variations on the analysis of vegetation change (Helsel and Hirsch, 2002), annual mean VAPs and greenness values were calculated for each lake to detect interannual changes, and linear regressions were performed among the 15-year annual mean data to obtain the annual rates of change in the VAP and the greenness values during the study period. The rate of change was considered statistically significant when the p-value associated with the linear regressions was < 0.05 (*t*-test). The 15-year climatologies of the VAPs and greenness values were estimated for each lake as the mean values of the 15 annual means between 2000 and 2014.

3.5. Validation of the wetland vegetation classification

To validate the accuracy of the vegetation delineation obtained using the 250-m resolution MODIS 8-day composed products, vegetation classified using concurrent higher-resolution (30-m) Landsat data was obtained, and the producer's/user's accuracies were estimated (Olofsson et al., 2014). The validation processes were as follows: (1) Landsat surface reflectance images were first masked using a MODIS-derived boundary for each lake, and > 30 samples for each cover types within the boundary were selected through visual interpretation of the RGB true color images (same as MODIS, the Landsat images were classified into three types: vegetation, water and mudflat), the spectral profiles, as well as concurrent high-resolution Google Earth images. The training samples then served as inputs for the Support Vector Machine (SVM) tool in the ENVI software to train a classifier, which was then used to classify the Landsat data of the entire region within the boundary. Indeed, the SVM classifier for Landsat could effectively distinguish vegetation from the other land cover types with an accuracy level of > 95% (Han et al., 2015; Feng et al., 2016). (2) Such classification processes were repeated for the 25 examined lakes for both dry and wet seasons. Then, 5000 random vegetation samples were selected from the Landsat classification maps for each lake, and were used as the 'truth' samples to gauge the accuracy of the concurrently (i.e., the same geographical location and acquisition time) MODIS classified vegetation with the estimated producer's accuracy and user's accuracy for each lake (Table 2).

The producer's accuracy ranged between 63.05% and 95.9% for the 25 lakes, with a mean value of 84.58 ± 0.09%, while the mean user's accuracy was 76.17 ± 0.08%, ranging from 61.19% to 91.23%. The different accuracy levels between these lakes were generally associated with the vegetation coverage. The percentage of mix-pixels tends to be larger for lakes with small areas of vegetation, causing smaller producer's accuracies. And the opposite is true for lakes with large vegetation coverage. These accuracy levels appear acceptable, considering the moderate spatial resolution of MODIS data (250 m) and various hydrological conditions of different lakes across such a large region. Note that the vegetation area delineated with the MODIS 8-day products represented the "mean" vegetation during the 8-day period, whereas the Landsat-derived results represented the conditions on a single day. Thus, the temporal differences between the observations made by the two satellites may lead to discrepancies among the corresponding vegetation results. Additionally, the mixing-pixel problem associated with the coarse resolution of MODIS data may serve as another reason for the misclassification, and better agreement could be expected once reliable un-mixing techniques are used.

3.6. Analysis of driving forces

The correlation analyses were performed to reveal the relationships between the explanatory variables (i.e., precipitation, sunshine hours, temperature, TSS) and vegetation greenness. The p-values (with *t*-test) were also estimated to determine whether the relationships were statistically significant (i.e., $p < 0.05$, *t*-test). Then, a multiple general linear model (GLM) regression analysis was conducted to quantify the relative contribution of each variable to interannual changes of the

Table 2
The vegetation classification accuracies of each lake using the phenology-based method.

Lake ID	Producer's accuracy	User's accuracy
L01	63.05%	87.21%
L02	93.84%	66.47%
L03	92.01%	90.06%
L04	78.14%	78.25%
L05	78.05%	69.12%
L06	88.94%	74.57%
L07	73.02%	76.27%
L08	74.25%	65.13%
L09	91.21%	67.49%
L10	93.94%	65.03%
L11	93.33%	61.19%
L12	83.5%	70.84%
L13	93.9%	83.07%
L14	94.57%	80.25%
L15	78.18%	80.45%
L16	91.31%	84.86%
L17	81.2%	80.98%
L18	75.71%	69.93%
L19	84.54%	71.15%
L20	94.64%	91.23%
L21	86.38%	85.16%
L22	72.98%	80.88%
L23	95.9%	71.51%
L24	82.45%	75.06%
L25	79.34%	78.1%
Mean ± STD.	84.58 ± 0.09%	76.17 ± 0.08%

vegetation greenness (Tao et al., 2014). Also, a p-value was estimated for each variable with the multiple GLM model, where a p-value of < 0.05 shows that the contribution of such variable is statistically significant.

4. Results and discussion

4.1. Temporal and spatial distributions of wetland vegetation

On average, the coverages of wetland vegetation accounted for 16.78% (Datong Lake) to 58.89% (Chihu Lake) of the total areas of these 25 lakes during the period 2000 to 2014 (see bar charts in Fig. 4 and Table 1). 24% (6/25) of the climatological VAPs of these lakes were > 50%, and 72% (18/25) ranged between 20% and 50%. Only one lake showed a 15-year mean VAP < 20%. Trend analysis revealed the changing trend of annual VAP for each lake during the study period (Fig. 5), and the change rates for all the lakes are color shaded in Fig. 4 to show their spatial distributions. When the VAP change rate is classified into five levels, $< -3\%\ yr^{-1}$, $-3\% \sim -1.5\%\ yr^{-1}$. $-1.5\% \sim 0\ yr^{-1}$, $0 \sim 1.5\%\ yr^{-1}$, $> 1.5\%\ yr^{-1}$, the number of lakes corresponding to each level accounted for 8%, 24%, 36%, 16% and 16% of all 25 of the studied lakes, respectively. Similar to the results for the greenness, more than half of the lakes (17/25) showed decreasing trends in their VAPs, and the most significant VAP decrease was also found for Shijiu Lake (L07, which displayed a rate of change of $-7.1\%\ yr^{-1}$). Of the lakes that experienced decreasing trends, 7 were statistically significant (indicated as "↓" in Fig. 4 and as blue arrows in Fig. 5, $p < 0.05$), and this number is smaller than the number of lakes that displayed significant decreases in greenness (11 lakes). In contrast, 3 of the lakes displayed statistically significant increasing VAP trends (indicated as "↑" in Fig. 4 and as red arrows in Fig. 5, $p < 0.05$).

The seasonality of the VAPs for the selected lakes are illustrated in Fig. 6, with each grid representing the seasonal mean VAP for a particular lake. In general, for most of the lakes, the VAPs in the second and third quarters were higher than those that occurred during the first and fourth quarters. Specifically, the maximum VAPs typically occurred in the second and third quarters, which accounted for 36% and 56% of the total number of lakes, respectively. On the other hand, the minimum VAPs were observed in the first and fourth quarter, which represented 48% and 44% of the lakes, respectively.

4.2. Seasonal and interannual changes in vegetation greenness

The 15-year greenness (estimated from NDVI values) climatology of each lake is presented both in Table 1 and as a bar chart in Fig. 7. Specifically, 44% (11/25) of the lakes have 15-year mean greenness values of < 0.2, 52% (13/25) were between 0.2 and 0.3, and 4% (1/25) were > 0.3. The interannual changes in the vegetation greenness values are shown in Fig. 8, and the associated annual rates of change are shown by the colors displayed in Fig. 7. Classifying the rates of change of greenness into five levels, $< -0.03\ yr^{-1}$, $-0.03 \sim -0.015\ yr^{-1}$. $-0.015 \sim 0\ yr^{-1}$, $0 \sim 0.015\ yr^{-1}$, and $> 0.015\ yr^{-1}$, the percentages of the lakes that fall into each level are 24%, 16%, 28%, 24% and 8%, respectively. Well over half of the lakes (17/25) have demonstrated decreasing trends in their greenness values over the period of 2000–2014, and the most pronounced decrease was observed in Shijiu Lake ($-0.075\ yr^{-1}$). 11 of the lakes showed statistically significant decreasing trends in vegetation greenness values during 2000 and 2014

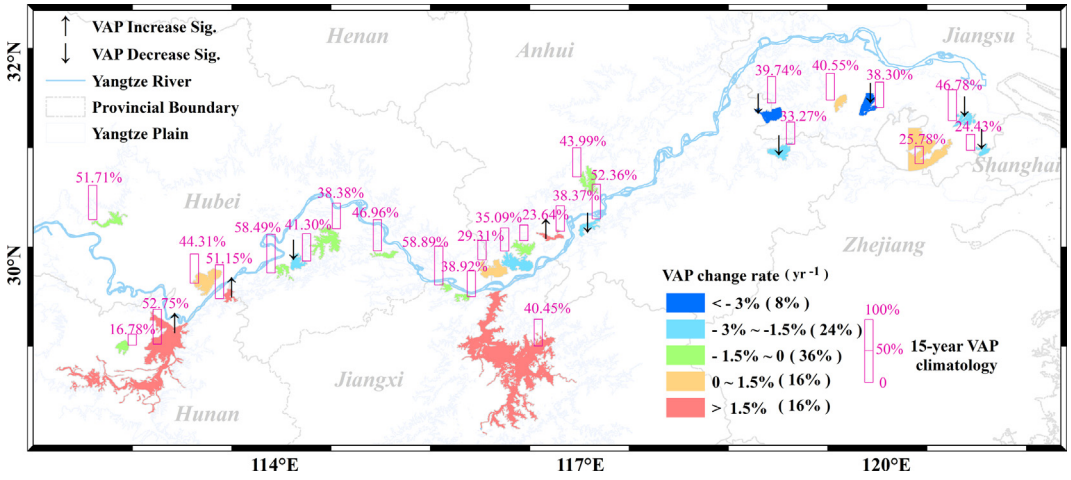

Fig. 4. The spatial distribution of the rate of change of the vegetation area percentage (VAP) for the 25 lakes examined, where '↑' and '↓' indicate that the VAPs exhibited statistically significant ($p < 0.05$) increasing or decreasing trends from 2000 to 2014, respectively. The numbers above the purple bars are the VAP climatologies of the lakes during the 15-year period. The numbers beside the legend in brackets are the percentages of the lakes that displayed the different rates of change over the 15-year period.

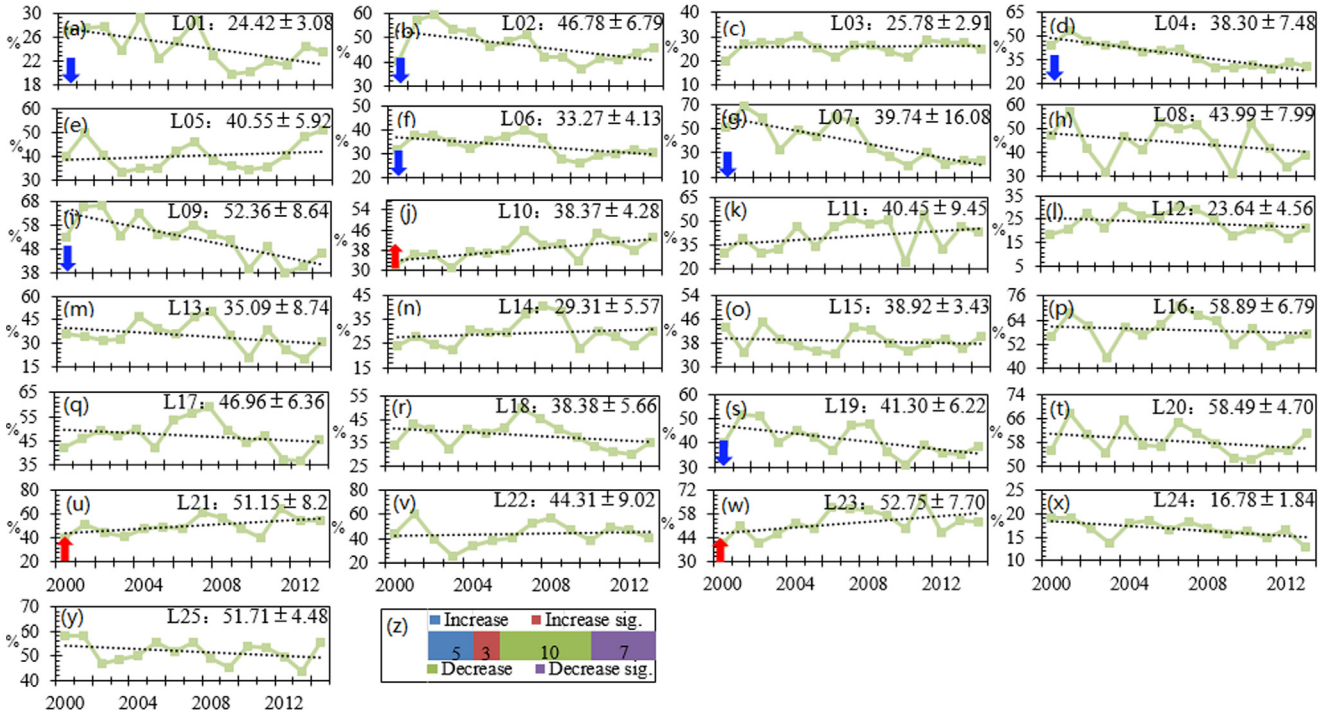

Fig. 5. The interannual vegetation area percentage (VAP) changes for each studied lake ((a)–(y)). The red and blue arrows indicate the lakes with significant ($p < 0.05$) increasing and decreasing trends in their VAPs over the 15 years. The numbers in the upper right corners of (a)–(y) represent the 15-year VAP climatologies and their standard deviations. (z) The numbers of lakes (annotated) that display increasing and decreasing VAPs and statistically significant ($p < 0.05$) decreasing and increasing trends in the study period of 2000–2014.

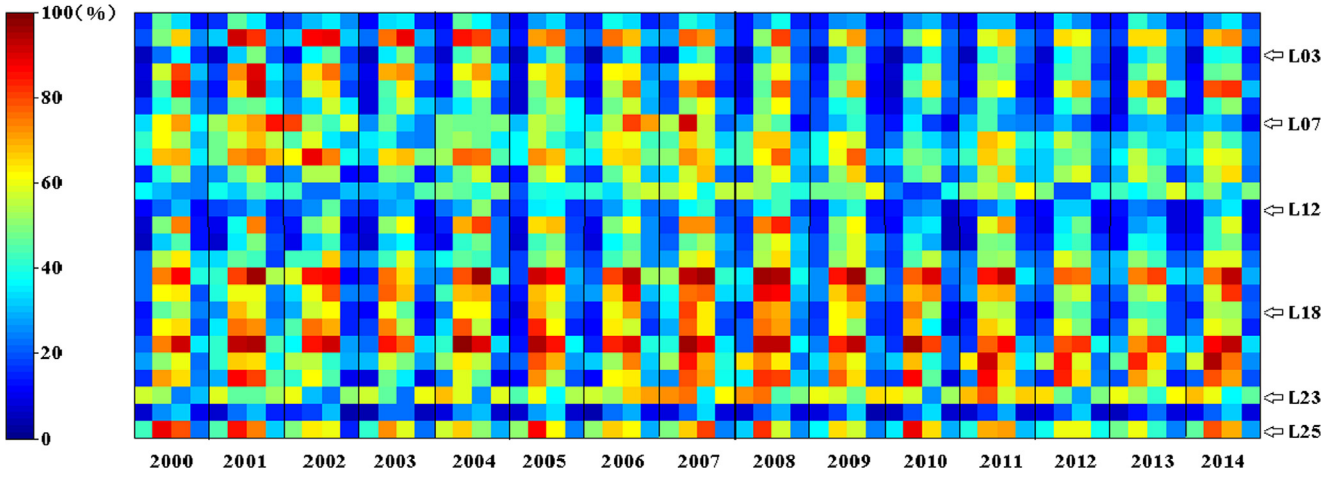

Fig. 6. Seasonal mean vegetation area percentages (VAPs) of the 25 lakes examined; each cell represents the seasonal mean VAP of a particular lake. The cells from top to bottom are consistent with the positions of the lakes from east to the west on the Yangtze Plain, and the codes (i.e., L03) correspond to those in Table 1, which are arranged by their longitudes.

(indicated as "↓" in Fig. 7 and as blue arrows in Fig. 8, $p < 0.05$), and most of them were located in the eastern Yangtze Plain (Fig. 7). On the other hand, statistically significant increasing trends in vegetation greenness values were observed in only 2 of the lakes (indicated as "↑" in Fig. 7 and as red arrows in Fig. 8, $p < 0.05$), and these lakes were found in the middle and western Yangtze Plain.

The seasonal mean vegetation greenness values for each lake are color coded in Fig. 9. The greenness values in the second and third quarters (greenish to reddish) are relatively higher than those that occur during the first and fourth quarters (bluish) for most of the lakes. The highest greenness values occurred in the third quarter for 84% of the total number of lakes, whereas the minimum NDVI values were observed in the first quarter for 68% of the lakes. Pronounced high vegetation was found in the second and third quarters of 2007 and 2008, especially for the lakes located in the middle and eastern Yangtze Plain.

4.3. Discussion

4.3.1. Driving forces

The correlations between the aforementioned five driving factors and the annual mean greenness values of all of the lakes were calculated (see Table 3). The responses of the annual mean vegetation greenness to the local fertilizer consumption varied among different lakes, where 20% (5/25) showed statistically significant ($p < 0.05$) positive correlations and 24% (6/25) of the lakes demonstrated

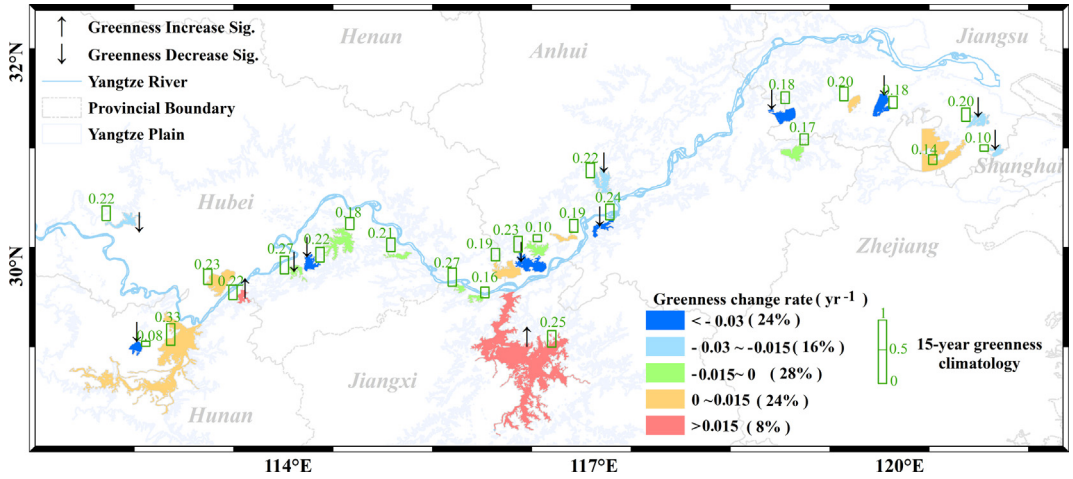

Fig. 7. The spatial distribution of the rate of change of the vegetation greenness values of the studied lakes. '↑' indicates lakes that displayed significant ($p < 0.05$) increasing trends in their vegetation greenness values, and '↓' indicates lakes that displayed significant ($p < 0.05$) decreasing trends from 2000 to 2014. The numbers above the bars are the 15-year vegetation greenness climatologies. The numbers beside the legend in brackets are the percentages of the lakes that displayed different rates of change.

negative correlations statistically significant ($p < 0.05$), respectively. The positive correlations may resulted from the favoring effects of the increasing of nutrients availability, while the growths of the vegetation for lakes with negative correlations could be inhibited by the high concentration of water fertility (Güsewell and Koerselman, 2002; Green and Galatowitsch, 2002), yet the exact reason for the different impacts require further investigation once more detailed regional data (instead of the total amounts of fertilizer consumption) are available.

The annual mean greenness values of most of the lakes (21/25) exhibited negative correlations with the regional precipitation, and this relationship was statistically significant ($p < 0.05$) for 32% (8/25) of the lakes. The vegetation greenness of 76% (19/25) of the lakes exhibited positive correlations with the regional temperature, where the relationship was statistically significant ($p < 0.05$) for 32% (8/25) of the lakes, highlighting the potential role of precipitation and temperature on the growth of vegetation in lake wetlands on the Yangtze Plain (Han et al., 2015; Zhang et al., 2017b). In contrast, both negative and positive correlations were found between the vegetation greenness and the daily sunshine, whereas the relationship appeared to be less significant than that of precipitation and temperature. On the other hand, the greenness values of 15 lakes showed negative correlations with the annual mean TSS, and 20% (5/25) of the lakes demonstrated

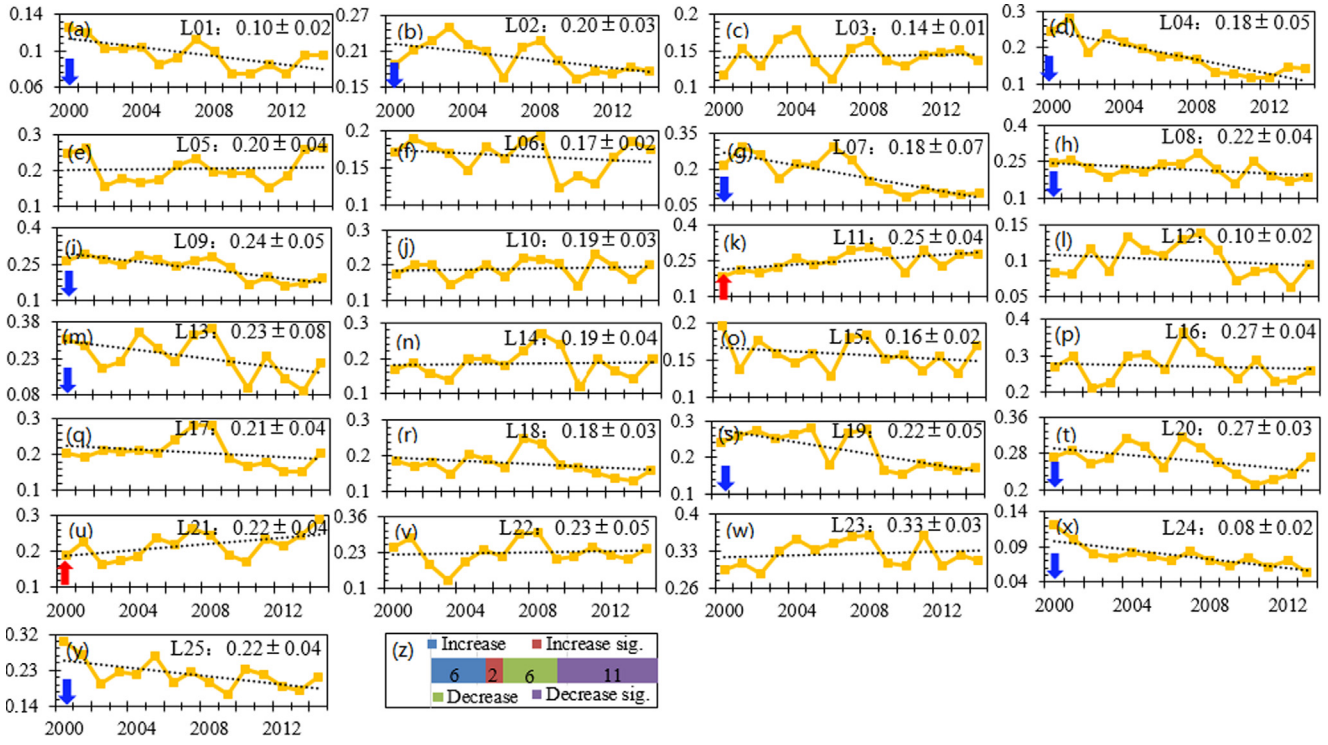

Fig. 8. The interannual changes in vegetation greenness values for each studied lake ((a)–(y)). The red and blue arrows indicate the lakes with significant ($p < 0.05$) increasing or decreasing trends in vegetation greenness values over the 15 years. The number in the upper right corners of (a)–(y) represent the 15-year greenness climatologies and the standard deviations. (z) The numbers of lakes (annotated) in which the greenness values decreased or increased and the numbers of lakes that displayed statistically significant ($p < 0.05$) decreasing or increasing trends during the study period (2000–2014).

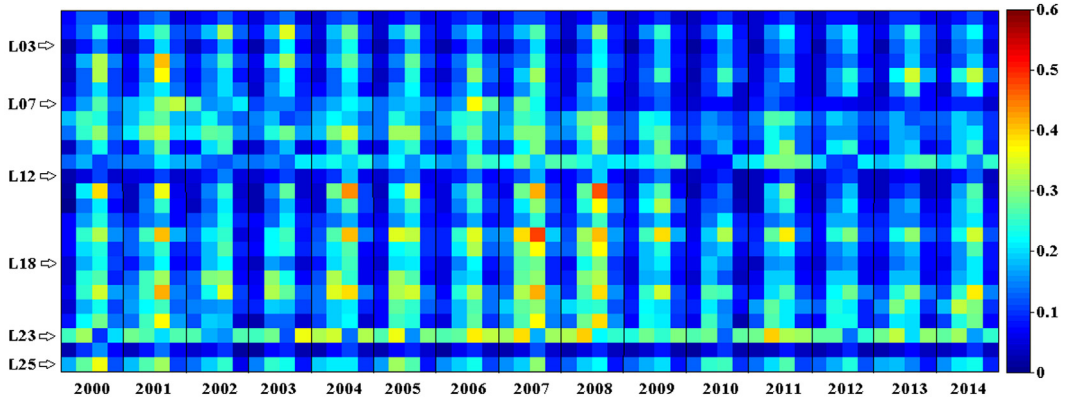

Fig. 9. Seasonal mean vegetation greenness values of the 25 lakes examined. Each cell represents the seasonal mean greenness of a given lake. From top to bottom, the cells follow the progression of the lakes from east to the west within the Yangtze Plain. The codes (i.e., L03) correspond to those in Table 1, which are arranged by their longitudes.

statistically significant ($p < 0.05$) negative correlations, indicating the importance of water clarity (e.g., light penetration) in modulating vegetation growth.

To further quantify the relative contributions of different driving factors to the wetland vegetation changes, a multiple general linear model (GLM) regression (Tao et al., 2014) was conducted using the associated annual data from 2000 to 2014. The contributions of the five drivers for all the 25 lakes are illustrated as percentages in Fig. 10 and Table 3, where the dominant factors for each lake are clearly revealed. The multiple GLM analyses shows that the amounts of chemical fertilizer consumption, precipitation, sunshine hours, temperature and TSS played the important roles in determining the interannual changes in wetland vegetation in 40% (10/25) , 12% (3/25) ,4% (1/25), 20% (5/25) and 12% (3/25) of the lakes, respectively. The combined contributions of the five factors explained 57.80% (L03, Taihu Lake) to 98.17% (L09, Shengjin Lake) of the interannual changes, with a mean value of 89.08 ± 7.89%. Indeed, the changes in annual vegetation greenness values in 17 of the lakes can be significantly ($p < 0.05$) explained by one or two of the five driving factors above (see Fig. 10). On the other hand, the residuals associated with the multiple GLM regressions accounted for over 40% of the variation in vegetation greenness in the lakes Taihu (L03), indicating that the changes in vegetation greenness in this lakes were likely controlled by other drivers.

4.3.2. *Limitations and future implications*

We acknowledge that the vegetation delineated using the MODIS data could have some problems with mixed pixels, and the signal associated with sparse vegetation may not be detectable using data with a resolution of 250 m. On the other hand, higher-resolution satellite images (such as the 30-m Landsat and 10-m SPOT images) are supposed to produce much more detailed vegetation classification maps than the moderate-resolution MODIS. The greater number of spectral bands of such instruments, rather than the two bands of MODIS, could also be used to construct more useful aquatic vegetation indices (such as

Table 3
Correlation coefficients (r) between the annual total fertilizer consumption amounts/annual mean precipitation/sunshine hour/temperature/ the annual mean water turbidity (TSS) and the annual mean greenness values of each lake. The contributions (Ctrb., in percentage) of the different driving factors to the interannual changes in the greenness values are also quantified and listed. Statistically significant ($p < 0.05$) correlation coefficients and contributions are annotated with an asterisk (*).

Code	Precipitation		Sunshine		Temperature		TSS		Fertilizer		Residuals
	r	Ctrb.	r	Ctrb.	r	Ctrb.	r	Ctrb.	r	Ctrb.	Ctrb.
L01	−0.15	0.71	−0.54*	0.16	0.51*	21.67*	−0.49*	9.74	0.73*	64.93*	2.79
L02	−0.54*	49.25*	−0.47*	12.67	0.28	5.06	0.17	1.07	0.47*	23.27	8.68
L03	−0.22	29.23	0.22	16.08	0.14	2.85	−0.04	3.32	−0.12	6.32	42.19
L04	−0.34	0.15	−0.08	0.00	−0.20	9.01	−0.60*	61.81*	0.51*	20.10	8.93
L05	0.15	0.53	−0.08	2.65	0.26	12.45	−0.31	24.81	−0.12	40.03	19.53
L06	−0.39	18.08	−0.15	0.14	0.28	6.46	−0.49*	2.73	−0.58*	62.15*	10.45
L07	−0.55*	9.27	0.42	1.70	−0.07	7.17	0.51*	7.73	0.73*	70.07*	4.07
L08	−0.66*	38.75*	0.03	5.77	0.10	0.00	−0.04	35.86*	−0.37	16.94*	2.67
L09	−0.65*	6.49	−0.06	0.07	0.77*	24.79*	0.06	1.98	−0.75*	64.83*	1.83
L10	−0.35	22.88	−0.35	37.55	0.06	16.36	−0.08	2.60	−0.20	7.97	12.65
L11	−0.41	4.24	0.47*	5.61	0.51*	52.64	0.18	2.56	0.242	22.12	12.83
L12	−0.25	1.16	−0.32	7.94	0.66*	72.42*	0.04	0.27	−0.29	9.64	8.57
L13	−0.68*	46.27*	−0.02	7.59	0.53*	1.34	0.21	1.13	−0.49*	36.94*	6.73
L14	−0.43	39.50	−0.19	21.73	0.25	4.26	−0.07	1.79	−0.07	18.24	14.49
L15	0.08	1.55	−0.25	0.91	−0.14	0.75	−0.61*	81.81*	0.28	0.32	14.67
L16	−0.44	19.09	0.33	4.30	0.08	3.02	0.46*	48.80	0.04	8.62	16.17
L17	−0.35	31.64	0.26	0.86	0.26	0.14	−0.35	21.66	−0.33	36.30	9.41
L18	−0.34	0.32	0.20	8.30	0.64*	71.38*	−0.29	7.35	0.05	3.52	9.12
L19	−0.15	0.11	0.13	7.09	0.50*	10.68	−0.44*	17.17	−0.62*	58.50*	6.45
L20	−0.21	2.20	−0.03	10.97	0.63*	69.10*	0.07	0.05	−0.43	8.17	9.52
L21	−0.49*	30.47	−0.37	11.67	−0.06	3.59	−0.21	9.26	0.50*	38.56*	6.46
L22	−0.51*	36.79	−0.48*	39.61*	0.05	9.66	−0.41	4.49	0.30	1.96	7.50
L23	−0.55*	67.72	0.13	1.70	0.39	10.72	0.20	1.68	0.14	2.48	15.71
L24	0.09	5.44	−0.43	13.45	−0.33	2.50	0.16	0.57	−0.62*	68.16*	9.89
L25	−0.51*	8.93	−0.17	4.79	−0.11	5.24	−0.36	6.63	−0.57*	62.84*	11.57

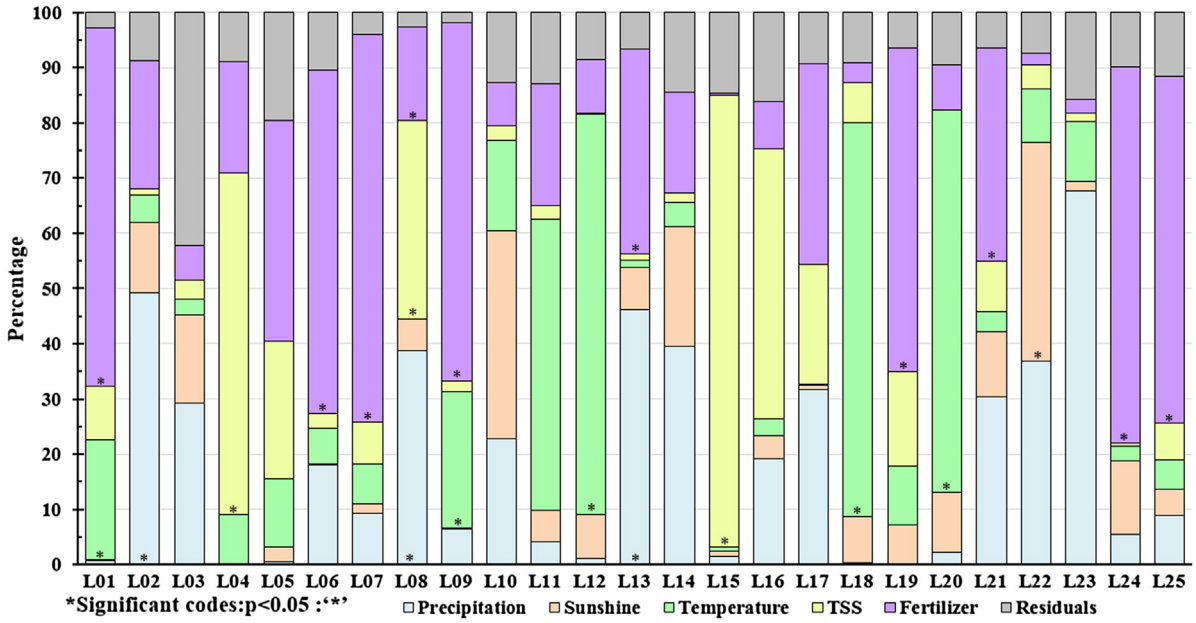

Fig. 10. The contributions of different driving factors (chemical fertilizer consumption, precipitation, sunshine hours, temperature and TSS) to the interannual changes in greenness values, expressed as percentages. Statistically significant contributions are annotated with an asterisk (*).

NDAVI and WAVI) for wetland vegetation detection (Villa et al., 2014). The main reason to use MODIS rather than Landsat or SPOT in this study was because due to the frequent clouds present over the Yangtze Plain region, the temporal distributions of cloud-free observations in different years may change significantly. Therefore, the interannual comparisons of vegetation coverage (VAP) or growing status (greenness) could be challenging, since the observed vegetation conditions among different years may hold various inundation conditions or phenological stages. In contrast, MODIS has daily global coverage, where the 8-day composites represent the best possible observational conditions during each 8-day period (e.g., small viewing angle, without clouds or cloud shadows, and low aerosol loading), providing statistically meaningful datasets to avoid potential seasonal sampling bias that may result from infrequent observations. Indeed, the vegetation classified using the MODIS and Landsat data agreed well, with an accuracy level ~80%, further confirming the fidelity of the results obtained from moderate resolution data.

Floating algae on the water surface may also show high NDVI values, interfering with the remote sensing-based classification of wetland vegetation (Oyama et al., 2015; Villa et al., 2015). In particular, when algae are present in one location for more than one month, the associated annual NDVI curve may resemble that of Category III (see Fig. 2a). The affected pixel could be misclassified as vegetation, leading to overestimation of the vegetation area during seasons that feature algae blooms. Such phenomena often occur over the entire extent of Chaohu Lake and certain portions of Taihu Lake in the Yangtze Plain (Hu et al., 2010; Zhang et al., 2015). In this study, we excluded Chaohu Lake and the western portion of Taihu Lake because the study of wetland vegetation in these two regions requires more advanced classification methods, while for the short-term (no more than one month) algae blooms in other lakes will be precluded.

The current study treated all vegetation communities as one class, in fact, using the phenological information to explore the spatial and temporal variance of different communities could be more important. For example, accurate assessments of wetland biodiversity changes and their transitions require community-level vegetation information (Ma et al., 2008; Luo et al., 2016; Luo et al., 2017). However, the first challenge in carrying out this task is to develop a sophisticated remote sensing classification method that includes a comprehensive understanding of the phenological features, living conditions, and other characteristics of different vegetation types in different lakes.

The amounts of chemical fertilizer, three meteorological factors and water turbidity were taken as the possible driving indicators in this research and their potential impacts on the interannual change of vegetation greenness for all lakes were investigated, however, other additional factors, such as levee construction, should ideally be investigated. In fact, the recent increase in vegetation in the two largest lakes connected to the Yangtze River (Poyang and Dongting Lakes) may also be associated with the impoundment of the Three Gorges Dam (TGD) upstream. Studies have shown that the inundation areas of these two lakes decreased in the post-TGD period, whereas the exposure time of the floodplain increased. These changes favor the growth of wetland vegetation and have led to prominent expansion of the vegetated areas (Xie et al., 2014; Han et al., 2015; Feng et al., 2016; Han et al., 2018). And the water level could also serve as another important factor modulating the growth of aquatic vegetation (Zhao et al., 2012), however, it appears impossible to obtain historical water level data for all lakes (as hydrological gauge stations are not available for most lakes) that cover the 15-year period examined in this study to assess their effects on vegetation change, thus, more localized efforts are required to investigate the contribution of water level to vegetation dynamics.

5. Conclusions

Using 15 years of NDVI time series data from MODIS and a phenology-based classification method, the spatial distributions and temporal dynamics of wetland vegetation in 25 large lakes on the Yangtze Plain were documented and analyzed. Phenological information from annual NDVI datasets were used to classify vegetation within a year, and then, the inter-annual variability and change trends of vegetation coverage and greenness between 2000 and 2014 were analyzed. This study presents two important findings that appear to have been previously unknown. First, more than half of the 25 lakes showed decreasing trends in their vegetation areas and greenness values over the 15-year period of 2000–2014. Seven and 11 of these lakes exhibited statistically significant decreasing trends in their VAPs and vegetation greenness values, respectively. In contrast, the number of lakes with increasing trends in vegetation was much less. Only 2 of the lakes demonstrated statistically significant increases in their annual mean

greenness values. Second, changes in consumption of chemical fertilizer for farmland, precipitation, daily sunshine hours, temperature and water turbidity played important roles in controlling the variability in the greenness values in 40%, 12%, 4%, 20% and 12% of the total number of lakes, respectively. In addition, the interannual trends in vegetation growth in 17 of the 25 lakes could be significantly ($p < 0.05$) explained by one or two of the five driving factors (consumption of chemical fertilizer for farmland, precipitation, daily sunshine hours, temperature and water turbidity).

The results of this study provide the first baseline datasets of the wetland vegetation changes that have occurred in 25 large lakes on the Yangtze Plain, the findings here could serve as important references for future environmental monitoring and restoration efforts of these lake wetlands.

Acknowledgements

This work was supported by the National Natural Science Foundation of China (NOs: 41671338, 41401388, 41331174 and 41706194), the Key Program of the Chinese Academy of Sciences (ZDRW-ZS-2017-3-4), the Guangdong Provincial Key Laboratory of Soil and Groundwater Pollution Control (No. 2017B030301012), the Strategic Priority Research Program of Chinese Academy of Sciences (No. XDA20060402), and the Open Fund of the State Key Laboratory of Lake Science and Environment (NO: 2016SKL001). Additional support was provided by the Southern University of Science and Technology (Grant No. G01296001). We thank NASA providing the MODIS surface reflectance data and TRMM precipitation products, the USGS for providing the Landsat surface reflectance data, the China Meteorological Data Sharing Service System for providing the meteorological data and Dr. Shengli Tao of Peking University for providing the calculation method for variables contribution in R.

References

Anhui, S.B., 2001–2015. Anhui Statistical Yearbook. China Statistics Press, Beijing, China.
Betbeder, J., Rapinel, S., Corgne, S., Pottier, E., Hubert-Moy, L., 2015. TerraSAR-X dual-pol time-series for mapping of wetland vegetation. ISPRS J. Photogramm. Remote Sens. 107, 90–98.
Cai, X., Feng, L., Hou, X., Chen, X., 2016. Remote sensing of the water storage dynamics of large lakes and reservoirs in the Yangtze River Basin from 2000 to 2014. Sci. Rep. 6, 1–9.
Chen, B., Chen, L., Huang, B., Michishita, R., Xu, B., 2018. Dynamic monitoring of the Poyang Lake wetland by integrating Landsat and MODIS observations. ISPRS J. Photogramm. Remote Sens. 139, 75–87.
Deng, F., Wang, X., Cai, X., Li, E., Jiang, L., Li, H., Yan, R., 2014. Analysis of the relationship between inundation frequency and wetland vegetation in Dongting Lake using remote sensing data. Ecohydrology 7, 717–726.
Dronova, I., Gong, P., Wang, L., Zhong, L., 2015. Mapping dynamic cover types in a large seasonally flooded wetland using extended principal component analysis and object-based classification. Remote Sens. Environ. 158, 193–206.
Duan, Z., Bastiaanssen, W.G.M., Liu, J., 2012. Monthly and annual validation of TRMM Mulitisatellite Precipitation Analysis (TMPA) products in the Caspian Sea Region for the period 1999–2003, International Geoscience and Remote Sensing Symposium (IGARSS), 2012, IEEE.
Feng, L., Han, X., Hu, C., Chen, X., 2016. Four decades of wetland changes of the largest freshwater lake in China: possible linkage to the Three Gorges Dam? Remote Sens. Environ. 176, 43–55.
Feng, L., Hu, C., Chen, X., Cai, X., Tian, L., Gan, W., 2012a. Assessment of inundation changes of Poyang Lake using MODIS observations between 2000 and 2010. Remote Sens. Environ. 121, 80–92.
Feng, L., Hu, C., Chen, X., Tian, L., Chen, L., 2012b. Human induced turbidity changes in Poyang Lake between 2000 and 2010: observations from MODIS. J. Geophys. Res. 117, 1–19.
Güsewell, S., Koerselman, W., 2002. Variation in nitrogen and phosphorus concentrations of wetland plants. Perspect. Plant Ecol. Evol. System. 5 (1), 37–61.
Green, E.K., Galatowitsch, S.M., 2002. Effects of Phalaris arundinacea and nitrate-N addition on the establishment of wetland plant communities. J. Appl. Ecol. 39 (1), 134–144.
Guo, L., 2007. Doing battle with the green monster of Taihu Lake. Science 317, 1166.
Han, X., Chen, X., Feng, L., 2015. Four decades of winter wetland changes in Poyang Lake based on Landsat observations between 1973 and 2013. Remote Sens. Environ. 156 426 417.
Han, X., Feng, L., Hu, C., Chen, X., 2018. Wetland changes of China's largest freshwater lake and their linkage with the Three Gorges Dam. Remote Sens. Environ. 204, 799–811.
Helsel, D., Hirsch, R., 2002. Statistical Methods in Water Resources Techniques of Water Resources Investigations. U.S. Geological Survey. 522 pages.
Hou, X., Feng, L., Duan, H., Chen, X., Sun, D., Shi, K., 2017. Fifteen-year monitoring of the turbidity dynamics in large lakes and reservoirs in the middle and lower basin of the Yangtze River, China. Remote Sens. Environ. 190, 107–121.
Houlahan, J.E., Keddy, P.A., Makkay, K., Findlay, C.S., 2006. The effects of adjacent land use on wetland species richness and community composition. Wetlands 26, 79–96.
Hu, C., Lee, Z., Ma, R., Yu, K., Li, D., Shang, S., 2010. Moderate Resolution Imaging Spectroradiometer (MODIS) observations of cyanobacteria blooms in Taihu Lake, China. J. Geophys. Res. 115, 1–20.
Hunan, S.B., 2001–2015. Hunan Statistical Yearbook. China Statistics Press, Beijing, China.
Hunbei, S.B., 2001–2015. Hubei Rural Statistical Year Book. China Statistics Press: Beijing, China.
Jeppesen, E., Sondergaard, M., Sondergaard, M., Christofferson, K., 1998. The Structuring Role of Submerged Macrophytes in Lakes, Ecological Studies. Springer Verlag.
Jiangsu, S.B., 2001–2015. Jiangsu Statistical Yearbook. China Statistics Press, Beijing, China.
Jiangxi, S.B., 2001–2015. Jiangxi Statistical Yearbook. China Statistics Press, Beijing, China.
Jing, R., Gong, Z., Zhao, W., Pu, R., Deng, L., 2017. Above-bottom biomass retrieval of aquatic plants with regression models and SfM data acquired by a UAV platform – a case study in Wild Duck Lake Wetland, Beijing, China. ISPRS J. Photogramm. Remote Sens. 134, 122–134.
Laba, M., Blair, B., Downs, R., Monger, B., Philpot, W., Smith, S., Sullivan, P., Baveye, P.C., 2010. Use of textural measurements to map invasive wetland plants in the Hudson River National Estuarine Research Reserve with IKONOS satellite imagery. Remote Sens. Environ. 114, 876–886.
Li, F., Li, C., Xiao, B., Wang, Y., 2013. Mapping large-scale distribution and changes of aquatic vegetation in Honghu Lake, China, using multitemporal satellite imagery. J. Appl. Remote Sens. 7 073593–073591–073593-073515.
Liu, T., Abd-Elrahman, A., 2018. Deep convolutional neural network training enrichment using multi-view object-based analysis of Unmanned Aerial systems imagery for wetlands classification. ISPRS J. Photogramm. Remote Sens. 139, 154–170.
Liu, X., He, L., Zhou, C., 2008. Study on lake surface area change in the mid-lower reaches of Yangtze River based on the remote sensing technique. J. East China Normal Univ. (Nature Sci.) 4, 124–129.
Liu, X., Zhang, S., Su, W., 1981. Application of Landsat images to the investigation of reed resources of Dongting Lake. Scientia Geographica Sinica 1 (1), 52–57.
Luo, J., Duan, H., Ma, R., Jin, X., Li, F., Hu, W., Shi, K., Huang, W., 2017. Mapping species of submerged aquatic vegetation with multi-seasonal satellite images and considering life history information. Int. J. Appl. Earth Observ. Geoinf. 57, 154–165.
Luo, J., Li, X., Ma, R., Lia, F., Duan, H., Hu, W., Qin, B., Huang, W., 2016. Applying remote sensing techniques to monitoring seasonal and interannual changes of aquatic vegetation in Taihu Lake, China. Ecol. Ind. 60, 503–513.
Ma, R., Duan, H., Gu, X., Zhang, S., 2008. Detecting aquatic vegetation changes in Taihu Lake, China using multi-temporal satellite imagery. Sensors 8, 3988–4005.
Martin, S., L.Johansson, L., L.Lauridsen, T., Jørgensen, T.B., Liboriussen, L., Jeppesen, E., 2010. Submerged macrophytes as indicators of the ecological quality of lakes. Freshw. Biol. 55, 893–908.
Maxa, M., Bolstad, P., 2009. Mapping northern wetlands with high resolution satellite images and LiDAR. Wetlands 29 (1), 248–260.
Olofsson, P., Foody, G.M., Herold, M., Stehman, S.V., E.Woodcock, C., Wulder, M.A., 2014. Good practices for estimating area and assessing accuracy of land change. Remote Sens. Environ. 148, 42–57.
Oyama, Y., Matsushita, B., Fukushima, T., 2015. Distinguishing surface cyanobacterial blooms and aquatic macrophytes using Landsat/TM and ETM+ shortwave infrared bands. Remote Sens. Environ. 157, 35–47.
Ozge, K.D., Akyurek, Z., Beklioglu, M., 2009. Identification and mapping of submerged plants in a shallow lake using quickbird satellite data. J. Environ. Manage. 90, 2138–2143.
Patel, V.M., Dholakia, M.B., Ray, S.S., 2015. Remote sensing techniques for land use/land cover mapping in Mahi Right Bank Canal command area, Gujarat. J. Civ. Eng. Technol. 2 (2), 01–10.
Sand-Jensen, K., Riis, T., Vestergaard, O., Larsen, S.E., 2000. Macrophyte decline in Danish lakes and streams over the past 100 years. J. Ecol. 88, 1030–1040.
Scheffer, M., Hosper, S.H., Meijer, M.-L., Moss, B., Jeppesen, E., 1993. Alternative equilibria in Shallow lakes. Trends Ecol. Evol. 8 (8), 275–279.
Secretariat, R.C., 2013. The Ramsar Convention Manual: a Guide to the Convention on Wetlands (Ramsar, Iran, 1971), sixth ed. Ramsar Convention Secretariat, Gland, Switzerland, p. 21.
Short, F.T., Kosten, S., Morgan, P.A., Malone, S., Moore, G.E., 2016. Impacts of climate change on submerged and emergent wetland plants. Aquat. Bot. 135, 3–17.
Song, X., Cai, X., Wang, Z., Li, E., Wang, X., 2016. Cummunity change of dominant submerged macrophyte in Lake Honghu since 1950s. J. Lake Sci. 28 (4), 859–867.
Szantoi, Z., Escobedo, F., Abd-Elrahman, A., Smith, S., Pearlstine, L., 2013. Analyzing fine-scale wetland composition using high resolution imagery and texture features. Int. J. Appl. Earth Observ. Geoinf. 23, 204–212.
Szantoi, Z., J.Escobedo, F., Abd-Elrahman, A., Pearlstine, L., Dewitt, B., Smith, S., 2015. Classifying spatially heterogeneous wetland communities using machine learning algorithms and spectral and textural features. Environ. Monit. Assess. 187, 1–15.
Tao, S., Fang, J., Zhao, X., Zhao, S., Shen, H., Hu, H., Tang, Z., Wang, Z., Guo, Q., 2014. Rapid loss of lakes on the Mongolian Plateau. PNAS 112 (7), 2281–2286.
Verhoef, W., 1996. Application of harmonic analysis of NDVI time series (HANTS). Fourier analysis of temporal NDVI in the Southern African and American continents.

Fourier analysis of temporal NDVI in the Southern African and American continents, pp. 19–24.
Villa, P., Bresciani, M., Bolpagni, R., Pinardi, M., Giardino, C., 2015. A rule-based approach for mapping macrophyte communities using multi-temporal aquatic vegetation indices. Remote Sens. Environ. 218–233.
Villa, P., Bresciani, M., Braga, F., Bolpagni, R., 2014. Comparative assessment of broadband Vegetation Indices over aquatic vegetation. IEEE J. Sel. Top. Appl. Earth Obs. Remote Sens. 7 (7), 1–17.
Wang, J., Sheng, Y.D., Tong, T.S., 2014. Monitoring decadal lake dynamics across the Yangtze Basin downstream of Three Gorges Dam. Remote Sens. Environ. 152, 251–269.
Wang, J., Sheng, Y., Wada, Y., 2017. Little impact of the Three Gorges Dam on recent decadal lake decline across China's Yantze Plain. Water Resour. Res. 53, 3854–3877.
Wang, P., Bao, W., 2010. Wetland information extraction from RS image based on wavelet packet and the active learning support vector machine. Comput. Comput. Technol. Agric. 346, 491–499.
Wang, S., Dou, H., 1998. Chinese Lake Cataloges. Science Press, Beijing.
Wu, W., 1977. Preliminary Investigation on the distribution of Vegetation and Oncomelania hupensis in Poyang Lake. J. Nanchang Univ. (Natural Sci.) (in Chinese).
Xiao, D., Zhang, C., Tian, K., Liu, G., Yang, H., An, S., 2015. Development of alpine wetland vegetation and its effect on carbon sequestration after dam construction: a case study of Lashihai in the northwestern Yunnan plateau in China. Aquat. Bot. 126, 16–24.
Xie, C., Huang, X., Mu, H., Yin, W., 2017. Impacts of Land Use Changes on the Lakes across the Yangtze Floodplain, China. Environ. Sci. Technol. 51 (7), 3669–3677.
Xie, Y.H., Yue, T., Xinsheng, C., Feng, L., Zhengmiao, D., 2014. The impact of Three Gorges Dam on the downstream eco-hydrological environment and vegetation distribution of East Dongting Lake. Ecohydrol.
Yu, K., Hu, C., 2013. Changes in vegetative coverage of the Hongze Lake national wetland nature reserve: a decade-long assessment using MODIS medium-resolution data. J. Appl. Remote Sens. 7 073589-073581-073589-073512.
Zhang, T., Ban, X., Wang, X., Li, E., Yang, C., Zhang, A.Q., 2016a. Spatial relationships between submerged aquatic vegetation and water quality in Honghu lake, China. Fresenius Environ. Bull. 25, 896–909.
Zhang, Y., Jeppesen, E., Liu, X., Qin, B., Shi, K., Zhou, Y., Thomaz, S.M., Deng, J., 2017a. Global loss of aquatic vegetation in lakes. Earth Sci. Rev. 179, 250–265.
Zhang, Y., Liu, X., Qin, B., Shi, K., Deng, J., Zhou, Y., 2016b. Aquatic vegetation in response to increased eutrophication and degraded light climate in Eastern Lake Taihu: implications for lake ecological restoration. Sci. Rep. 6 (23867), 1–12.
Zhang, Y., Ma, R., Zhang, M., Duan, H., Loiselle, S., Xu, J., 2015. Fourteen-Year Record (2000–2013) of the spatial and temporal dynamics of floating algae blooms in Lake Chaohu, observed from time series of MODIS images. Remote Sens. 7, 10523–10542.
Zhang, Y., Yang, N., Xu, J., Yin, Y., 2017b. Long-term study of the relationship between precipitation and aquatic vegetation succession in east Taihu Lake, China. Scientifica 2017, 1–8.
Zhao, D., Jiang, H., Cai, Y., An, S., 2012. Artificial regulation of water level and its effect on aquatic macrophyte distribution in Taihu Lake. PLoS ONE 7, e44836.
Zhejiang, S.B., 2001–2015. Zhejiang Statistical Yearbook. China Statistics Press, Beijing, China.